Table I

reaction	rate constant[a]	ref
(1) $H\cdot + O_2 \rightarrow HO_2\cdot$	2×10^{10}	3
(2) $H\cdot + H\cdot \rightarrow H_2$	2.2×10^{10}	3
(3) $H\cdot + \cdot OH \rightarrow H_2O$	1.5×10^{10}	3
(4) $H\cdot + HO_2\cdot \rightarrow H_2O_2$	1.3×10^{10}	3
(5) $\cdot OH + HO_2\cdot \rightarrow H_2O + O_2$	1.18×10^{10}	3
(6) $\cdot OH + \cdot OH \rightarrow H_2O_2$	1.2×10^{10}	3
(7) $HO_2\cdot + HO_2\cdot \rightarrow H_2O_2 + O_2$	2.1×10^{6}	3
(8) $OH + Cl^- \rightarrow OH^- + Cl\cdot$	4.3×10^{9}	4
(9) $H\cdot + H_2O_2 \rightarrow H_2O + \cdot OH$	6×10^{7}	5
(10) $Cl\cdot + Cl^- \rightarrow Cl_2^{-}\cdot$	2.1×10^{10}	4
(11) $Cl_2^{-}\cdot \rightarrow Cl\cdot + Cl^-$	1.1×10^{5}	4
(12) $Cl_2^{-}\cdot + Cl_2^{-}\cdot \rightarrow Cl_3^- + Cl^-$	4.0×10^{9}	1
(13) $Cl_2^{-}\cdot + HO_2\cdot \rightarrow 2Cl^- + H^+ + O_2$	1.0×10^{9}	1
(14) $Cl_2^{-}\cdot + H\cdot \rightarrow 2Cl^- + H^+$	7×10^{9}	1
(15) $H_2O_2 + Cl_2^{-}\cdot \rightarrow HO_2\cdot + 2Cl^- + H^+$	1.4×10^{5}	6
(16) $Cl_2 + Cl^- \rightarrow Cl_3^-$	1.8×10^{5}	7
(17) $Cl_3^- \rightarrow Cl_2 + Cl^-$	1.0×10^{6}	7
(18) $Cl_2 + HO_2\cdot \rightarrow Cl_2^{-}\cdot + H^+ + O_2$	see text	
(19) $Cl_3^- + HO_2\cdot \rightarrow Cl_2^{-}\cdot + Cl^- + H^+ + O_2$	see text	

[a] Rate constants for reactions of the type $R\cdot + R\cdot \rightarrow$ products are those defined by $-d[R\cdot]/dt = k[R\cdot]^2$. The units are $M^{-1}\ s^{-1}$ except for reactions 11 and 17 where they are s^{-1}.

reaction scheme 1-19. The fit shown in Figure 2 is good. By comparison with previous work,[1] it is clear that reaction 18 makes little difference to the decay of $Cl_2^{-}\cdot$.

We conclude that $HO_2\cdot$ reduces Cl_2 with $k = 1.0 \times 10^9\ M^{-1}\ s^{-1}$, i.e., close to the diffusion-controlled limit. The reaction may take place in various circumstances and should, for example, be considered together with some of the other reactions in Table I when formulating free-radical mechanisms for the reaction between H_2O_2 and Cl_2.[12,13]

Acknowledgment. This work was partly supported by grants from the Cancer Research Campaign and the Medical Research Council.

(12) Davies, G.; Kustin, K. *Inorg. Chem.* **1973**, *12*, 961.
(13) Held, A. M.; Halko, D. J.; Hurst, J. K. *J. Am. Chem. Soc.* **1978**, *100*, 5732.

Resonance Raman Evidence of Iron Pentacoordination in High-Spin Ferric Cytochrome P-450. A Comparison with Model Compound Iron(III) Protoporphyrin IX Dimethyl Ester *p*-Nitrobenzenethiolate

Pavel Anzenbacher,* Zdeněk Šípal, and Bohuslav Strauch[†]

Department of Biochemistry, Charles University Albertov 2030, 128 40 Prague 2, Czechoslovakia

Jacek Twardowski and Leonard M. Proniewicz[‡]

Institute of Zoology, Jagellonian University Karasia 6, 30060 Cracow, Poland

Received March 4, 1981
Revised Manuscript Received July 6, 1981

The resonance Raman (RR)[1] spectra of biomolecules provide an unique in situ insight into the stereochemistry of these substances.[2-4] Recently, Spiro et al.[5] reported in this journal a well-documented analysis of RR spectra of various heme proteins and their model substances. These data demonstrate that from the positions of high-frequency RR bands information about heme coordination and porphyrin core expansion can be drawn. As has been shown by structural studies, the central iron atom in high-spin ferric porphyrin complexes may be either five- or six-coordinated.[6,7] Spiro et al.[5] have presented reasoning which allows one to check the probability of iron penta- or hexacoordination in this class of heme compounds. Similar conclusions were reached also by Sievers et al.[8] The data presented in ref 5 support previous suggestions that porphyrin core expansion is responsible for the decrease of RR band frequencies of heme compounds (Spaulding et al.[9], Huong and Pommier[10]). From the position of spin-sensitive RR bands (marked II, IV, and V[11]), a porphyrin center-to-pyrrole nitrogen distance (C_t-N) can be calculated from the equation[5,10] $\nu = KA - Kd$, where d is the C_t-N distance in Å, ν the Raman shift frequency in cm^{-1}, and the constants K (cm^{-1}/Å) and A (Å) are 375.5 and 6.01 for band II, 555.6 and 4.86 for band IV, and 423.7 and 5.87 for band V, respectively. These relations were used to probe heme expansion in various heme proteins and model complexes.[5,9,10,12] The correlation for band V has been found to be less satisfactory due to contributions from various porphyrin-ring-stretching vibrations.[12a]

This procedure can be applied to the interpretation of the RR pattern of cytochrome P-450, a heme protein acting as a terminal oxidase in monooxygenation of a variety of both foreign and endogeneous substrates.[13] For a better understanding of its mode of action, the question of axial ligands of heme iron atom is of paramount importance. There is a strong indirect evidence of

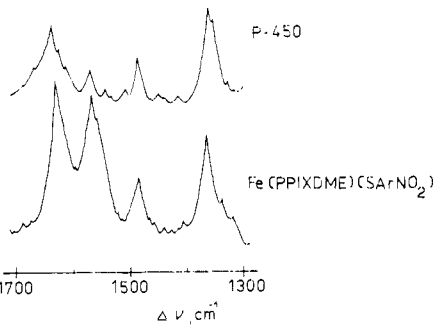

Figure 1. RR spectra of rat LM HS P-450 and model substance Fe(PPIXDME)($SArNO_2$). Model compound prepared according to ref 15. For preparation of P-450, see original work.[16c] Excitation wavelength, 488.0 nm; average incident power, 100 mW. Rat LM HS P-450: Jeol JRS S1 spectrometer, slit width 8.4 cm^{-1}, scan rate 60 cm^{-1}/min, sample in capillary (see ref 16c); Fe(PPIXDME)($SArNO_2$): Cary 82 spectrometer, slit width 7 cm^{-1}, scan rate 36 cm^{-1}/min, sample with KBr (1:1 w/w).

[†] Department of Inorganic Chemistry.
[‡] Central Laboratory for Physicochemical Analyses and Structural Research.

(1) Abbreviations used: RR, resonance Raman; P-450, Cytochrome P-450; HS, high spin; LS, low spin; Fe(PPIXDME)($SArNO_2$), iron(III) protoporphyrin IX dimethyl ester *p*-nitrobenzenethiolate; LM, liver microsomes; cam, P-450 from bacteria *Pseudomonas putida* grown on camphor; HRP, horseradish peroxidase; $(Me_2SO)_2$Fe(PPIX), bis(dimethyl sulfoxide) iron(III) protoporphyrin IX dimethyl ester; $(Me_2SO)_2$Fe(OEP), its octaethylporphyrin analogue; MetHb, methemoglobin; $(Im)_2$Fe(MP), bis(imidazole)iron(III) mesoporphyrin.

(2) Spiro, T. G. *Biochim. Biophys. Acta* **1975**, *416*, 169-189.
(3) Warshel, A. *Annu. Rev. Biophys. Bioeng.* **1977**, *6*, 273-300.
(4) Carey, P. R. *Q. Rev. Biophys.* **1978**, *11*, 309-370.
(5) Spiro, T. G.; Stong, J. D.; Stein, P. *J. Am. Chem. Soc.* **1979**, *101*, 2648-2655.
(6) Zobrist, M.; LaMar, G. N. *J. Am. Chem. Soc.* **1978**, *100*, 1944-1946.
(7) Mashiko, T.; Kastner, M. E.; Spartalian, K.; Scheidt, W. R.; Reed, C. A. *J. Am. Chem. Soc.* **1978**, *100*, 6354-6362.
(8) Sievers, G.; Österlund, K.; Ellfolk, N. *Biochim. Biophys. Acta* **1979**, 581, 1-14.
(9) Spaulding, I. D.; Chang, C. C.; Yu, N.-T.; Felton, R. H. *J. Am. Chem. Soc.* **1975**, *97*, 2517-2525.
(10) Huong, P. V.; Pommier, J. C. *C. R. Hebd. Seances Acad. Sci., Ser. C* **1977**, *285*, 519-522.
(11) Spiro, T. G.; Burke, J. M. *J. Am. Chem. Soc.* **1976**, *98*, 5482-5489.
(12) (a) Lanir, A.; Yu, N.-T.; Felton, R. H. *Biochemistry* **1979**, *18*, 1656-1660. (b) Asher, S. A.; Schuster, T. M. *Ibid.* **1979**, *18*, 5377-5387. (c) McCandlish, E.; Miksztal, A. R.; Nappa, M.; Sprenger, A. Q.; Valentine, J. S.; Strong, J. D.; Spiro, T. G. *J. Am. Chem. Soc.* **1980**, *102*, 4268-4271. (d) Campbell, J. R.; Clark, R. J. H.; Clore, G. M.; Lane, A. N. *Inorg. Chim. Acta* **1980**, *46*, 77-84. (e) Armstrong, R. S.; Irwin, M. J.; Wright, P. E. *Biochem. Biophys. Res. Commun.* **1980**, *95*, 682-689.
(13) (a) Estabrook, R. W. *Methods Enzymol.* **1978**, *52*, 43-47. (b) Gunsalus, I. C.; Sligar, S. G. *Adv. Enzymol.* **1978**, 47, 1-44. (c) White, R. E.; Coon, M. J. *Annu. Rev. Biochem.* **1980**, *49*, 315-356.

0002-7863/81/1503-5928$01.25/0

Table I. Resonance Raman Band Positions, Iron Coordination Numbers, and C_t–N Distances in Ferric Heme Proteins and Model Systems[a]

compd	ref	band II, cm^{-1}	band IV, cm^{-1}	coord no.	C_t–N, Å
	High Spin				
chlorhemin	9	1495	1572	5	2.03
Fe(PPIXDME)($SArNO_2$)	this work	1490	1572	5	2.03
P-450 (rat, LM)	16c	1490	1578	5	2.03
P-450 (rabbit, LM)	16b		1571	5	2.03
P-450 (cam, bacteria)	16a	1488	1570	5	2.04
HRP native	18, 19	1500	1575	5	2.02
cytochrome c'	20, 21	1500	1578	5	2.02
$(Me_2SO)_2$Fe(PPIX)	5	1475	1560	6	2.06
$(Me_2SO)_2$Fe(OEP)	5	1481	1563	6	2.06
fluoride HRP	18, 19	1482	1555	6	2.06
MetHb	5	1481	1561	6	2.06
	Low Spin				
$(Im)_2$Fe(MP)	9, 11	1505	1584	6	2.00
cyanide HRP	18	1497	1590	6	2.01
cytochrome c	12a	1506	1585	6	2.00
P-450 (rat, LM)	16c, 22	1505	1580	6	2.00
P-450 (rabbit, LM)	16b	1502	1585	6	2.01
P-450 (cam, bacteria)	16a	1502	1581	6	2.01

[a] For abbreviations, see ref 1.

thiolate sulfur coordinated in the 5th coordination position, mainly on the basis of spectral studies of model compounds.[14] Among those model substances, the Fe(PPIXDME)($SArNO_2$)[1] gives the closest approach to the optical, EPR, and Mössbauer spectral properties of high-spin (HS)[1] ferric cytochrome P-450.[15] Because the question of possible hexacoordination in high-spin ferric heme proteins is still a subject of discussion[5-8,13c] the possibility of proving the iron pentacoordination in HS P-450[1] by RR spectroscopy using the reasoning quoted above is, in the absence of direct crystallographic data, attractive.

To this purpose we have measured the RR spectrum of Fe(PPIXDME)($SArNO_2$) as a pentacoordinated HS model compound with a thiolate axial ligand and compared it with that of HS P-450 reported by us and other authors.[16] The RR spectra of HS P-450 from rat liver microsomes[16c] and of the model compound are displayed in Figure 1; the positions of important RR bands (II and IV) of various HS and LS heme proteins and model substances are summarized in Table I. The comparison of the values shows clearly that the HS P-450 is similar to the Fe(PPIXDME)($SArNO_2$) and behaves like a five-coordinated HS iron(III) heme protein.

The average values of the C_t–N distance, calculated according to the above-mentioned relationship, are also included in Table I. The distance of 2.03 Å, found for both HS P-450 and Fe(PPIXDME)($SArNO_2$), is somewhat greater than that determined for the latter compound by crystallographic analysis (2.017 Å).[15] This slight discrepancy observed with nonplanar hemes was discussed in the original paper.[5] The calculated C_t–N distance for cytochrome P-450 fits also well to the family of pentacoordinated HS hemes.[5,9,18-21] The average C_t–N values for LS P-450 correspond well to the value of 2.00 Å, found by Cramer et al.[17] for rabbit LS P-450 with an extended X-ray absorption fine-structure technique (EXAFS).

The results presented thus give a strong support to the hypothesis of thiolate ligation in P-450 and iron pentacoordination in high-spin ferric P-450, which is the crucial point for understanding the P-450 enzyme mechanism because of low-spin/high-spin equilibrium modulation caused by binding of substrate. Moreover, the resonance Raman data also supply a reasonable estimate of the porphyrin ring radius in this heme protein.

Acknowledgment. This work was supported partly by agreement between Charles University, Prague, and Jagellonian University, Cracow.

(14) Chang, C. K.; Dolphin, D. *Bioorg. Chem.* **1978**, *4*, 37–80. Ruf, H. H; Wende, P.; Ullrich, V. J. *Inorg. Biochem.* **1979**, *11*, 189–204. Berzinis, A. P.; Traylor, T. G. *Biochem. Biophys. Res. Commun.* **1979**, *87*, 229–235.
(15) Tang, S. C.; Koch, S.; Papaefthymiou, G. C.; Foner, S.; Frankel, R. B.; Ibers, J. A.; Holm, R. H. *J. Am. Chem. Soc.* **1976**, *98*, 2414–2434.
(16) (a) Champion, P. M.; Gunsalus, I. C.; Wagner, G. C. *J. Am. Chem. Soc.* **1978**, *100*, 3743–3751. (b) Ozaki, Y.; Kitagawa, T.; Kyogoku, Y.; Imai, Y.; Hashimoto-Yutsudo, C.; Sato, R. *Biochemistry* **1978**, *17*, 5826–5831. (c) Anzenbacher, P.; Šípal, Z.; Chlumský, J.; Strauch, B. *Stud. Biophys.* **1980**, *78*, 73–74.
(17) Cramer, S. P.; Dawson, J. H.; Hodgson, K. O.; Hager, L. P. *J. Am. Chem. Soc.* **1978**, *100*, 7282–7290.
(18) Rakshit, G.; Spiro, T. G. *Biochemistry* **1974**, *13*, 5317–5323.
(19) Remba, R. D.; Champion, P. M.; Fitchen, D. B.; Chiang, R.; Hager, L. P. *Biochemistry* **1979**, *18*, 2280–2290.
(20) Kitagawa, T.; Ozaki, Y.; Kyogoku, T.; Horio, T. *Biochim. Biophys. Acta* **1977**, *495*, 1–11.
(21) Strekas, T. C.; Spiro, T. G. *Biochim. Biophys. Acta* **1974**, *351*, 237–245.
(22) Anzenbacher, P.; Šípal, Z.; Strauch, B., unpublished data.

An Organosilicon Polymer That Is Derived from a Mineral and Is at Least Partly Ladderlike and Inherently Fibrous

Jesse Hefter and Malcolm E. Kenney*

Department of Chemistry, Case Western Reserve University Cleveland, Ohio 44106

Received September 8, 1980

We report herein a polymer that is at least partly ladderlike and inherently fibrous. This polymer is a siloxane and has pendent trimethylsilyl and silanol groups. The route used to make it involves the synthesis of a silicate containing the polymeric ladder ion shown in Figure 1a and then the silylation of this ion.

The silicate which has been employed the most for the synthesis of this polymer is litidionite, $NaKCuSi_4O_{10}$. A drawing showing the specific structural arrangement of the ladder ion in this silicate[1] is presented in Figure 1b.

The litidionite was made by placing a disk of a sodium–potassium–copper glass of appropriate stoichiometry on a thin bed of previously prepared and powdered litidionite and then heating this assemblage. It was also made by sintering a mixture of Na_2CO_3, K_2CO_3, CuO, and SiO_2 having the appropriate stoichiometry.[2-5]

Because of the nature of these procedures, it is apparent that the processes occurring in them which lead to the formation of the silicate ion are mainly ion migration processes. In the devitrification procedure these processes are probably integral parts of the crystallization process. In the sintering procedure this is certainly the case.

The silylated polymer was prepared from the litidionite by exposing a piece of it to a stirred mixture of trimethylchlorosilane, water, and dioxane. The polymer was also prepared by using mixtures of trimethylchlorosilane, water, and acetone or tetrahydrofuran and using powdered instead of lump litidionite.[6] It was purified by washing and density separation techniques.

(1) Martin Pozas, J. M.; Rossi, G.; Tazzoli, V. *Am. Mineral.* **1975**, *60*, 471.
(2) Hydrothermal methods for making litidionite have been reported: (a) Guth, J.-L.; Kalt, A.; Perati, B.; Wey, R. *C. R. Hebd. Seances Acad. Sci., Ser. D* **1977**, 285, 1221. (b) Kawamura, K.; Kawahara, A. *Acta Crystallogr., Sect. B* **1977**, *33B*, 1071.
(3) Natural litidionite occurs in exceedingly tiny amounts in association with a blue glass found in the crater of Mt. Vesuvius: Zambonini, F. "Mineralogia Vesuviana"; S.I.E.M.: Naples, 1935; p 435.
(4) It is likely that the devitrification procedure parallels the process leading to natural litiodionite.
(5) The sintering procedure is similar to that used to make cuprorivaite, $CaCuSi_4O_{10}$: Pabst, A. *Acta Crystallogr.* **1959**, *12*, 733.
(6) These procedures are patterned after earlier mineral silylation and germylation procedures. See, for example: (a) Lentz, C. W. *Inorg. Chem.* **1964**, *3*, 574. (b) Frazier, S. E.; Bedford, J. A.; Hower, J.; Kenney, M. E. *Ibid.* **1967**, *6*, 1693. (c) Calhoun, H. P.; Masson, C. R. *J. Chem. Soc., Chem. Commun.* **1978**, 560.

0002-7863/81/1503-5929$01.25/0